Available online at www.sciencedirect.com

SciVerse ScienceDirect

Ceramics International 38 (2012) 6585–6590

CERAMICS INTERNATIONAL

www.elsevier.com/locate/ceramint

Enhanced ethanol gas sensing properties of SnO_2 nanobelts functionalized with Au

Changhyun Jin[a], Hyunsu Kim[a], Sunghoon Park[a], Hyoun Woo Kim[b], Sangmin Lee[c], Chongmu Lee[a,*]

[a]*Department of Materials Science and Engineering, Inha University, 253 Yonghyun-dong, Nam-gu, Incheon 402–751, Republic of Korea*
[b]*Division of Materials Science and Engineering, Hanyang University, 17 Haengdang Dong, Seongdong Gu, Seoul 133–791, Republic of Korea*
[c]*Department of Electronic Engineering, Inha University, 253 Yonghyun-dong, Nam-gu, Incheon 402–751, Republic of Korea*

Received 3 May 2012; received in revised form 13 May 2012; accepted 14 May 2012
Available online 22 May 2012

Abstract

SnO_2 nanobelts functionalized with Au were prepared using a three-step process consisting of the thermal evaporation of Sn powders, sputter deposition of Au, and annealing. Multiple-networked sensors were fabricated using Au-functionalized SnO_2 nanobelts. Scanning electron microscopy revealed nanobelts with widths ranging from a few hundred nanometers to a few micrometers, thicknesses of a few hundred nanometers, and lengths ranging from a few to a few tens of micrometers coated with the Au nanoparticles with a mean diameter of ~200 nm. The bare SnO_2 nanobelts showed responses of 2.80 and 2.20% to C_2H_5OH concentrations of 50 and 100 ppm, respectively. In contrast, the Au-functionalized SnO_2 nanobelts showed responses of 313.25 and 194.77%, respectively, to the same C_2H_5OH concentrations. Furthermore, SnO_2 nanobelts functionalized with Au showed a higher response than those functionalized with other metal catalysts, such as Pd, Pt and Ag. Both the response and recovery times of the SnO_2 nanobelts were decreased slightly by Au-functionalization regardless of the C_2H_5OH concentration. In addition, this paper discusses the enhanced sensing properties of SnO_2 nanobelts functionalized with Au.

Keywords: A. Powders: B. Electron microscopy; E. Sensors; gas phase reaction

1. Introduction

Ethanol sensors are commonly applied in the biomedical and chemical industries to assess wine quality, food degradation, to identify drunk drivers, and to monitor fermentation and other processes in chemical industries, etc. [1]. Metal oxide one-dimensional (1D) nanostructures, including SnO_2, ZnO, In_2O_3 and TiO_2, have been studied for general-purpose gas sensor applications because 1D nanostructure sensors offer the advantages of higher sensitivity, shorter response and recovery times and lower cost than the thin film-type sensors owing to their high surface-to-volume ratios [2–6]. Among these metal oxides, SnO_2 may be the most widely used material for gas sensing due to the high mobility of conduction electrons, and good chemical and thermal stability under the operating conditions of sensors [7,8]. This sensing performance can be enhanced further by incorporating a surface functionalization technique into their simple 1D nanostructure sensors [9]. Noble metal catalysts, such as Pd, Pt, Au, and Ag, have been used for functionalization to enhance the interaction of the target gas with the oxygen absorbed on the surface [10–13]. This paper reports the synthesis, structure and C_2H_5OH gas sensing properties of n-type SnO_2 nanobelts functionalized with Au. The results obtained in this study were compared with those obtained previously using SnO_2 nanowires functionalized with Pt [14] and Ag [15]. The origin of the enhanced sensing properties of n-type SnO_2 nanobelts by functionalization with Au is also discussed.

2. Experimental procedure

SnO_2 1D nanostructures were synthesized on Au-coated p-type Si (1 0 0) substrates by the thermal evaporation of Sn

*Corresponding author. Tel.: +82 32 860 7536; fax: +82 32 862 5546.
E-mail address: cmlee@inha.ac.kr (C. Lee).

0272-8842/$36.00
http://dx.doi.org/10.1016/j.ceramint.2012.05.043

powders. An aluminum boat containing the Sn powders was placed in the middle of a quartz tube inserted in a horizontal tube furnace. An Au-coated Si substrate was placed above the boat with the deposition side faced downwards. Before deposition, the tube was evacuated to 0.01 Torr using a rotary pump. The furnace was heated to 900 °C and maintained at that temperature for 2 h under a total gas pressure of 1 Torr. The furnace was then cooled to room temperature. Subsequently, a thin Au film was deposited onto the surface of some of the SnO_2 nanobelt samples by direct current (DC) magnetron sputtering (substrate temperature: room temperature, power: 100 W, current: 20 mA, working pressure: 1.9×10^{-2} Torr, and process time: 180 s). The Au-coated nanobelts were annealed at 700 °C for 30 min in an Ar atmosphere. The Ar gas flow rate and process pressure were 100 standard cubic centimeters per minute (sccm) and 0.8 Torr, respectively.

The Au-coated nanobelts were then annealed at 800 °C in an Ar atmosphere for 30 min to make an Au layer into discrete nanoparticles. The collected nanobelt samples were characterized by scanning electron microscopy (SEM, Hitachi S-4200) equipped with an energy dispersive X-ray spectrometer (EDXS), transmission electron microscopy (TEM, Philips CM-200) and X-ray diffraction (XRD, Philips X'pert MRD diffractometer).

For the sensing measurement, Ni (~200 nm in thickness) and Au (~50 nm) thin films were deposited sequentially by sputtering to form electrodes using an interdigital electrode mask. Fig. 1 shows a schematic diagram of the multiple-networked SnO_2 nanobelt sensors. The electrical and gas sensing properties of the as-synthesized and Au-functionalized SnO_2 nanobelts were measured at 100 °C using a home-made gas sensing measurement system. During the measurements, the nanobelt gas sensors were placed in a sealed quartz tube with an electrical feed through. A set amount of C_2H_5OH (>99.99%) gas was injected into the testing tube through a microsyringe to obtain C_2H_5OH concentrations of 50 and 100 ppm. At the same time, the electrical resistance of the nanobelts was monitored. The electrical resistance of the gas sensors was determined by measuring the electric current when a potential difference of 0.5 V was applied between the Ni/Au inter-digital electrodes (IDEs). The response of the n-type SnO_2 nanobelt sensors was defined as $(R_a - R_g)/R_g$ for the reducing gas, C_2H_5OH, where R_a and R_g are the electrical resistances of the sensors in air and target gas, respectively. The response time is defined as the time required for the change in electrical resistance to reach 90% of the equilibrium value after injecting the gas. The recovery time is defined as the time needed for the sensor to return to 90% above the original resistance in air after removing the gas.

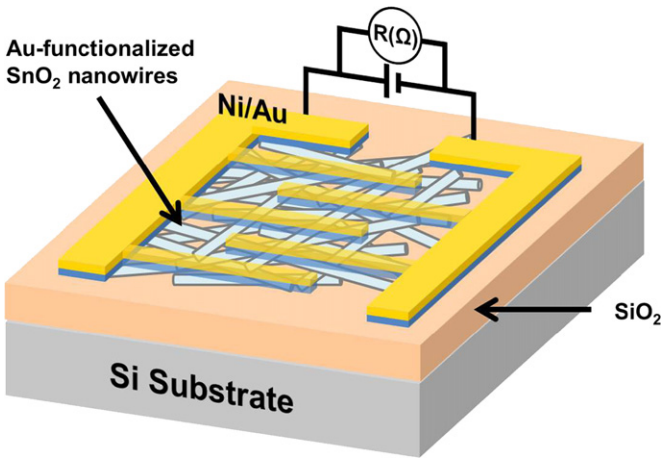

Fig. 1. Schematic diagram of a sensor fabricated with Au-functionalized SnO_2 nanobelts.

3. Results and discussion

Fig. 2(a) shows FE-SEM images of the Au-functionalized SnO_2 1D nanostructures prepared by a three-step process consisting of the thermal evaporation of Sn powders, sputter deposition of Au and thermal annealing. Scanning electron microscopy showed that SnO_2 nanobelts with widths ranging from a few hundred nanometers to a few micrometers, thicknesses of a few hundred nanometers, and lengths ranging from a few to a few tens of micrometers had been coated with Au nanoparticles with a mean diameter of ~200 nm. Au was detected in the EDX spectrum (Fig. 2(b)). The Cu detected in the EDX spectrum was not used as a catalyst but as a conductor for TEM sample preparation.

The crystal structures of the SnO_2 nanobelts functionalized with Au was examined by XRD (Fig. 2(c)). Most of the XRD peaks in the pattern fit the primitive tetragonal SnO_2. The low-magnification TEM image revealed SnO_2 nanobelts with a uniform width of approximately 500 nm and Au particles with a mean diameter of approximately 200 nm on the surface of the SnO_2 nanobelt (Fig. 2(d)). A SnO_2 single crystal nanobelt was observed on the left-hand side, whereas nanocrystalline Au was observed on the right hand side of the high-resolution TEM (HRTEM) image taken from the interface region of SnO_2 and Au (Fig. 2(e)). The reflection spots in the corresponding selected area electron diffraction (SAED) pattern (Fig. 2(f)) were identified as (1 1 0), (2 0 0) and (0 2 0) reflections of a primitive tetragonal-structured SnO_2 with lattice constants a= 0.4738 nm and c=0.3187 nm (JCPDS no. 41-1445), indicating that the SnO_2 nanobelt in the TEM image is a single crystal. No reflection spots from the Au nanoparticles were detected, presumably because the refection spots were too dim to be detected. The lack of Au reflection spots in the SAED pattern (Fig. 2(f)) indicates that most of the Au nanoparticles might be amorphous, but the fringe pattern in the HRTEM image of the particle (Fig. 2(e)) revealed the Au particle to be comprised mainly of nanocrystalline face-centered cubic Au. The resolved spacings between two neighboring parallel fringes were approximately 0.33 and 0.24 nm corresponding to the (1 1 0) and (2 0 0) lattice planes of primitive tetragonal SnO_2, respectively.

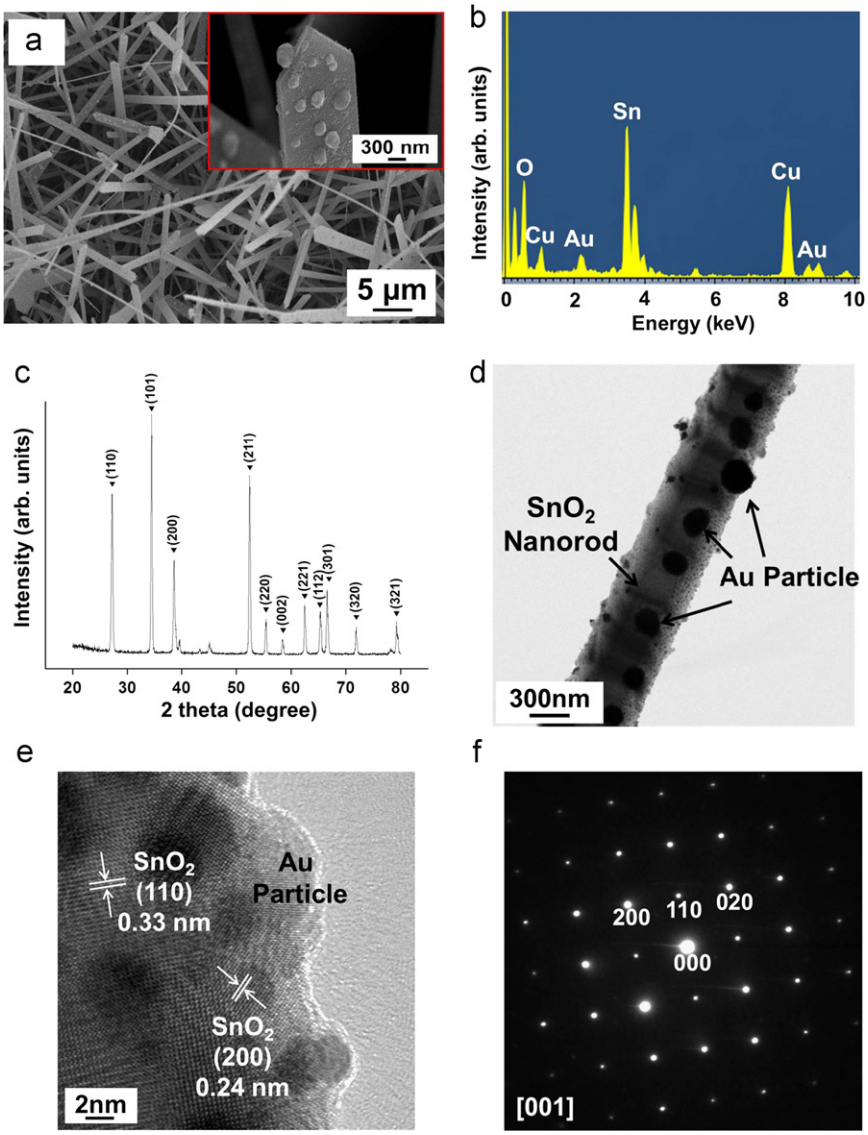

Fig. 2. (a) SEM image, inset, enlarged SEM image, (b) EDX spectrum, (c) XRD pattern of Au-functionalized SnO_2 nanobelts, (d) low-magnification TEM image of a typical Au-functionalized SnO_2 nanobelt, (e) high-resolution TEM and (f) corresponding SAED pattern of the SnO_2–Au interface region.

Fig. 3(a) shows the dynamic sensing characteristics of the multiple-networked bare SnO_2 nanobelts and Au-functionalized SnO_2 nanobelts to a reducing gas C_2H_5OH at 100 °C. Fig. 3(b) is simply the enlarged part of Fig. 3(a) at a C_2H_5OH concentration of 100 ppm drawn to show the moments of gas input and gas stop. The resistance responded well to C_2H_5OH gas. The resistance decreased rapidly when the nanobelt sensors were exposed to C_2H_5OH gas, and the resistance recovered completely to the initial value when the C_2H_5OH gas supply was stopped and air was introduced. Table 1 lists the responses measured from Fig. 3(a)–(d). The bare SnO_2 nanobelts showed responses of 2.80 and 2.20% at C_2H_5OH concentrations of 50 and 100 ppm, respectively. In contrast, the Au-functionalized SnO_2 nanobelts showed responses of 313.25 and 194.77%, respectively, to the same C_2H_5OH concentrations. Consequently, Au functionalization improved the responses of the nanobelts by approximately 112 and 89 times at 50 and 100 ppm C_2H_5OH, respectively (Table 1). Both the response and recovery times of SnO_2 nanobelts appeared to be decreased slightly by Au-functionalization regardless of the C_2H_5OH concentration (Table 1). Therefore, the functionalized nanobelt sensor was obviously superior to the bare SnO_2 nanobelt sensor in terms of both response and sensing speed. In addition, a comparison of the sensing properties of the Au-functionalized SnO_2 nanobelts in this study with those of Pt or Ag-functionalized SnO_2 1D nanostructures reported previously [14–20] indicates that Au functionalization is as efficient in improving the sensing properties of SnO_2 1D nanostructures as Pt- or Ag-functionalization (Table 2). The Au-functionalized SnO_2 nanobelts showed far higher responses than Pt-functionalized SnO_2 nanowires in sensing ethanol [14], even though the former

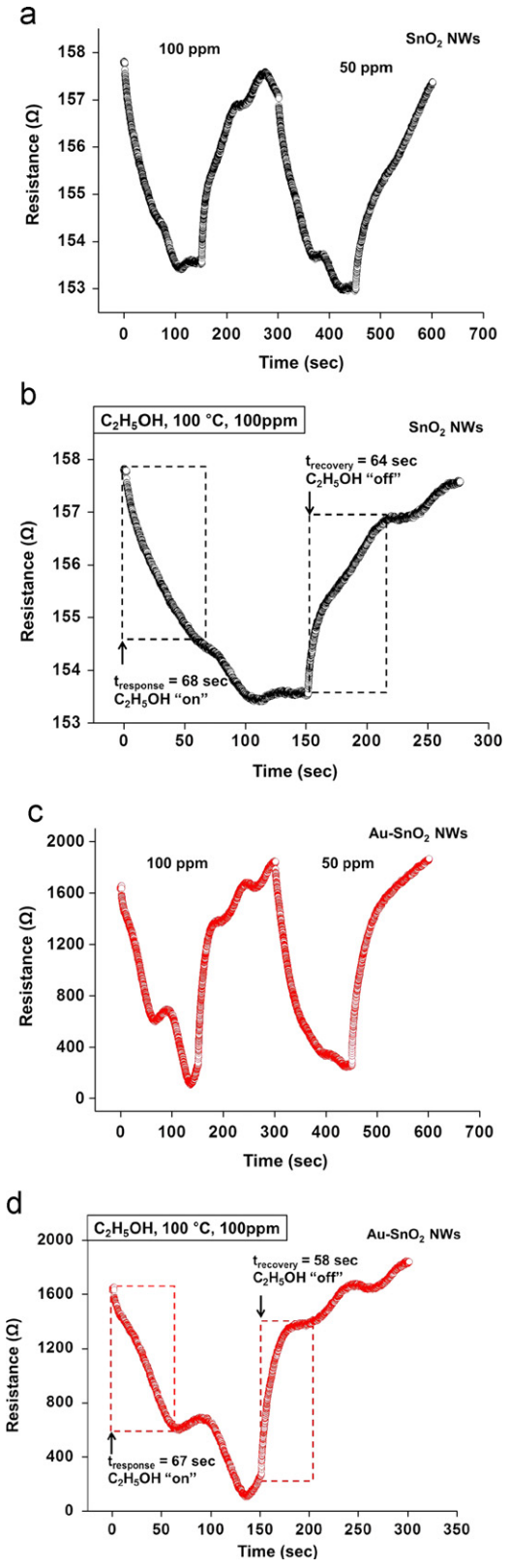

Fig. 3. Comparison of the dynamic response of an Au-functionalized SnO_2 nanobelt sensor with that of the bare SnO_2 nanobelt sensor. (a) Dynamic response of the bare SnO_2 nanobelt sensor. (b) Enlarged part of (a) at a C_2H_5OH concentration of 100 ppm drawn to reveal the moments of gas input and gas stop. (c) Dynamic response of the Au-functionalized SnO_2 nanobelt sensor. (d) Enlarged part of (c) at a C_2H_5OH concentration of 100 ppm drawn to reveal the moments of gas input and gas stop.

showed somewhat longer response and recovery times. The Au-functionalized SnO_2 nanobelts showed significantly higher responses as ethanol sensors than Ag-functionalized SnO_2 nanowires [15], even though the former showed longer recovery times.

When the SnO_2 sensing material is exposed to air, it interacts with oxygen by transferring electrons from the valence band to the adsorbed oxygen atoms, forming ionic species such as O^-, O^{2-} and O_2^-, as shown below [21].

$$O_2\ (g) \rightarrow O_2\ (ads) \quad (1)$$

$$O_2\ (ads) + e^- \rightarrow O_2^-\ (ads) \quad (2)$$

$$O_2^-\ (ads) + e^- \rightarrow 2O^-\ (ads) \quad (3)$$

$$O^-\ (ads) + e^- \rightarrow O_2^-\ (ads) \quad (4)$$

The potential barrier increases with increasing the number of oxygen ions on the surface, resulting in a higher resistance [22]. When the sensors are exposed to ethanol gas, which is a reducing gas, ethanol molecules react with oxygen ions to form CO_2 and H_2O according to the following reactions, and the electrons are released back into the nanobelts [23]:

$$CH_3CH_2OH\ (gas) \rightarrow CH_3CH_2OH\ (ads) \quad (5)$$

$$CH_3CH_2OH\ (ads) + 6O^-\ (ads) \rightarrow 2CO_2\ (gas) + 3H_2O\ (gas) + 6e^- \quad (6)$$

This leads to an increase in the carrier concentration of the sample and a decrease in depletion width. In other words, the depleted electrons are released back to the conduction band, which results in a sharp decrease in the resistance of the sensors. Such adsorbed oxygen and large surface-to-volume ratio increase the response of the SnO_2 nanobelt gas sensors. On the other hand, the nanobelt network probably increases the rate of oxygen adsorption and reduces the recovery time.

In the case of Au-functionalized SnO_2 nanobelts, the C_2H_5OH gas is spilt over the SnO_2 nanobelt surface by the Au nanoparticles [22], and the chemisorption and dissociation of C_2H_5OH gas [5] on the Au nanoparticle surface is enhanced owing to its high catalytic or conductive nature. Consequently, the number of electrons released from the gas species increases. In short, a combination of the spillover effect, enhancement of chemisorption and dissociation of gas, and the formation of electrons results in a higher electrical response of the Au-functionalized SnO_2 nanobelt sensor to C_2H_5OH gas.

4. Conclusions

SnO_2 nanobelts functionalized with Au were prepared using a three-step process consisting of the thermal evaporation of Sn powders, sputter-deposition of Au, and thermal annealing. Two different types of multiple-networked nanobelt sensors were fabricated using the bare and Au-functionalized SnO_2 nanobelts, respectively. The surface functionalized nanobelts with widths ranging from a few hundred nanometers to a few micrometers, thicknesses of a few hundred nanometers, and

Table 1
Responses, response times and recovery times measured at different C_2H_5OH concentrations for bare and Au-functionalized SnO_2 nanobelt sensors.

	Response (%)		Response time (s)		Recovery time (s)	
C_2H_5OH conc.	SnO_2	Au-SnO_2	SnO_2	Au-SnO_2	SnO_2	Au-SnO_2
100 ppm	2.20	194.77	68	67	64	58
50 ppm	2.80	313.25	82	61	62	51

Table 2
Comparison of the response, response time and recovery time of Au, Pt, Pd, and Ag-functionalized SnO_2 1D nanostructure sensors.

Nanostructures	Gas	Conc. (ppm)	Temp. (°C)	Response (%)	Response time (sec)	Recovery time (sec)	Refs.
Au-SnO_2 NWs	C_2H_5OH	50	100	313.25	61	51	Present work
	H_2S	20	400	380.9	1	214∼267	[16]
Pt-SnO_2 NWs	H_2	1000	100	118.0	–	–	[17]
	C_2H_5OH	500	200	22.0	2.0	4.2	[14]
	H_2	100	280	8.2	∼9	∼9	[18]
Pd-SnO_2 NWs	H_2	500	400	6	–	–	[19]
	CO	50	300	–	85	185	[20]
Ag-SnO_2 NWs	C_2H_5OH	100	450	228.1	∼80	0.4	[15]

lengths ranging from a few to a few tens of micrometers were coated with Au nanoparticles with a mean diameter of ∼200 nm. The nanobelts were primitive tetragonal-structured single crystal SnO_2. On the other hand, the Au nanoparticles were mainly amorphous but locally nanocrystalline. Au functionalization improved the responses of the SnO_2 nanobelts to C_2H_5OH by approximately 112 and 89 times at 50 and 100 ppm C_2H_5OH, respectively. Furthermore, the SnO_2 nanobelts functionalized with Au showed higher responses to C_2H_5OH than those functionalized with other metal catalysts, such as Pd, Pt, and Ag. Both the response and recovery times of the SnO_2 nanobelts were decreased by Au-functionalization regardless of the C_2H_5OH concentration. The functionalized nanobelt sensor was superior to the bare SnO_2 nanobelt sensor in terms of both response and sensing speed. The enhanced chemisorption of C_2H_5OH gas molecules and the formation of electrons by them enhances the electrical response of the Au-functionalized SnO_2 nanobelt sensor to C_2H_5OH gas.

Acknowledgment

This study was supported by the Key Research Institute Program through the National Research Foundation of Korea (NRF) funded by the Ministry of Education, Science and Technology (2011-0018394).

References

[1] A.W. Jones, Alcohol: Analysis—Wiley Encyclopedia of Forensic Science, John Wiley & Sons. Ltd., 2009.
[2] Q. Wan, J. Huang, Z. Xie, T.H. Wang, E.N. Dattoli, W. Lu, Branched SnO_2 nanowires on metallic nanowire backbones for ethanol sensor application, Applied Physics Letters 92 (2008) 102101.
[3] A. Kolmakov, Y. Zhang, G. Cheng, M. Moskovits, Detection of CO and O_2 using Tin oxide nanowire sensors, Advanced Materials 15 (2003) 997–1000.
[4] Y. Liu, E. Koep, M. Liu, A highly sensitive and fast-responding SnO_2 sensor fabricated by combustion chemical vapor deposition, Chemistry of Materials 17 (2005) 3997–4000.
[5] M. Law, H. Kind, B. Messer, F. Kim, P. Yang, Photochemical sensing of NO_2 with SnO_2 nanoribbon nanosensors at room temperature, Angewandte Chemie 114 (2002) 2511–2514.
[6] Y.H. Lin, M.W. Huang, C.K. Liu, J.R. Chen, J.M. Wu, H.C. Shih, The preparation and high photon-sensing properties of fluorinated tin dioxide nanowires, Journal of the Electrochemical Society 156 (2009) K196–K199.
[7] S. Habibzadeh, A.A. Khodadadi, Y. Mortazavi, CO and ethanol dual selective sensor of Sm_2O_3-doped SnO_2 nanoparticles synthesized by microwave-induced combustion, Sensors and Actuators B 144 (2010) 131–138.
[8] F. Pourfayaz, Y. Mortazavi, A. Khodadadi, S. Ajami, Ceria-doped SnO_2 sensor highly selective to ethanol in humid air, Sensors and Actuators B 130 (2008) 625–629.
[9] H. Chen, N. Xu, S. Deng, D. Lu, Z. Li, J. Zhou, J. Chen, Gasochromic effect and relative mechanism of WO_3 nanowire films, Nanotechnology 18 (2007) 205701.
[10] P. Bhattacharyya, P.K. Basu, C. Lang, H. Saha, S. Basu, Noble metal catalytic contacts to sol–gel nanocrystalline zinc oxide thin films for sensing methane, Sensors and Actuators B 129 (2008) 551–557.
[11] J.Q. Xu, J.J. Han, Y. Zhang, Y.A. Sun, B. Xie, Studies on alcohol sensing mechanism of ZnO based gas sensors, Sensors and Actuators B 132 (2008) 334–339.
[12] Z.P. Sun, L. Liu, L. Zhang, D.Z. Jia, Rapid synthesis of ZnO nanorods by one-step, room-temperature, solid-state reaction and their gas-sensing properties, Nanotechnology 17 (2006) 2266–2270.
[13] A.W. Warner, D.L. White, W.A. Bonner, Acoustooptic light deflectors using optical activity in paratellurite, Journal of Applied Physics 43 (1972) 4489–4495.

[14] Y.H. Lin, Y.C. Hsueh, P.S. Lee, C.C. Wang, J.R. Chen, J.M. Wu, T.P. Perng, H.C. Shih, Preparation of Pt/SnO_2 core-shell nanowires with enhanced ethanol gas- and photon-sensing properties, Journal of the Electrochemical Society 157 (2010) K206–K210.

[15] I.S. Hwang, J.K. Choi, H.S. Woo, S.J. Kim, S.Y. Jung, T.Y. Seong, I.D. Kim, J.H. Lee, Facile control of C_2H_5OH sensing characteristics by decorating discrete Ag nanoclusters on SnO_2 nanowire networks, **ACS** Applied Materials & Interfaces 3 (2011) 3140–3145.

[16] K.Y. Dong, J.K. Choi, I.S. Hwang, J.W. Lee, B.H. Kang, D.J. Ham, J.H. Lee, B.K. Ju, Enhanced H_2S sensing characteristics of Pt doped SnO_2 nanofibers sensors with micro heater, Sensors and Actuators B 157 (2011) 154–161.

[17] Y. Shen, T. Yamazaki, Z. Liu, D. Meng, T. Kikuta, Hydrogen sensors made of undoped and Pt-doped SnO_2 nanowires, Journal of Alloys and Compounds 488 (2009) L21–L25.

[18] H. Zhang, Z. Li, L. Liu, X. Xu, Z. Wang, W. Wang, W. Zheng, B. Dong, C. Wang, Enhancement of hydrogen monitoring properties based on Pd-SnO_2 composite nanofibers, Sensors Actuators B 147 (2010) 111–115.

[19] H. Huang, Y.C. Lee, C.L. Chow, C.Y. Ong, M.S. Tse, O.K. Tan, Pd surface modification of SnO_2-based nanorod arrays for H_2 gas sensors, IEEE Sensors 2008 Conference (2008) 114–117.

[20] M. Epifani, J. Arbiol, E. Pellicer, E. Comini, P. Siciliano, G. Faglia, J.R. Morante, Synthesis and gas-sensing properties of Pd-doped SnO_2 nanocrystals. A case study of a general methodology for doping metal oxide nanocrystals, Crystal Growth & Design 8 (2008) 1774–1778.

[21] O.V. Safonova, G. Delabouglise, B. Chenevier, A.M. Gaskov, M. Labeau, CO and NO_2 gas sensitivity of nanocrytalline tin dioxide thin films doped with Pd, Ru and Rh, Materials Science and Engineering C 21 (2002) 105–111.

[22] S.R. Morrison, Selectivity in semiconductor gas sensors, Sensors and Actuators B 12 (1987) 425–440.

[23] J. Li, H. Fan, X. Jia, W. Yang, P. Fang, Enhanced blue–green emission and ethanol sensing of Co-doped ZnO nanocrystals prepared by a solvothermal route, Applied Physics A 98 (2010) 537–542.